

On the Formation of C_{2v} - $C_{72}(11188)Cl_4$: A Particularly Stable Non-IPR Fullerene

Antonio Moreno-Vicente, Laura Abella, Khalid Azmani, Antonio Rodríguez-Forteza and Josep
M. Poblet**

Departament de Química Física i Inorgànica, Universitat Rovira i Virgili, c/Marcel·lí Domingo 1,
43007 Tarragona, Spain

Abstract

Halogenation has been one of the most used strategies to explore the reactivity of empty carbon cages. In particular, the higher reactivity of non-IPR fullerenes, i.e. those fullerenes that do not satisfy the Isolated Pentagon Rule (IPR), has been used to functionalize and capture these less stable fullerenes. Here, we have explored the stability of the non-IPR isomer $C_{72}(11188)$ with C_{2v} symmetry, which is topologically linked to the only IPR isomer of C_{70} , as well as its reactivity to chlorination. DFT calculations and Car-Parrinello molecular dynamics simulations suggest that chlorination takes place initially in non-specific sites, once carbon cages are formed. When the temperature in the arc-reactor decreases sufficiently, Cl atoms are trapped on the fullerene surface, migrating from not-so-favored positions to reach the most favored sites in the pentalene. We have also discussed why cage $C_{2v}\text{-}C_{72}(11188)$ is found to take four chlorines, whereas cage $C_1\text{-}C_{74}(14049)$ is observed to capture ten of them, despite these two fullerenes are closely related by a simple C_2 insertion.

1. Introduction

Since the initial discovery of C_{60}^+ ion in 1985,¹ an abnormally stable compound, many soccer-ball-shaped molecules have been synthesized and characterized.^{2,3} Classical fullerenes are spherical closed and empty carbon networks containing only hexagons and twelve pentagons. Most stable empty cages satisfy the well-known Isolated Pentagon Rule (IPR), C_{60} being its most iconic member.⁴ It was not until 2000 that the first carbon cages that violated the IPR rule were observed; $Sc_2@C_{66}$ ⁵ and $Sc_3N@C_{68}$,⁶ fullerenes encapsulating two metal ions and a trimetallic nitride, respectively. Nowadays, it is well-established that the instability coming from the adjacent pentagons can be counterbalanced by charge transfer from an encapsulated metal atom or cluster.^{7,8} Several carbon cages containing one, two or three adjacent pentagons have been reported so far; $Sc_2C_2@C_{68}(6073)$,⁹ $Sc_3N@C_{70}(7854)$,¹⁰ $Sc_2X@C_{70}(7892)$, ($X = S^{11}$ and O^{12}), $Sc_2S@C_{72}(10528)$,¹³ $La@C_{72}(10612)$,¹⁴ $La_2@C_{72}(10611)$,¹⁵⁻¹⁷ $DySc_2N@C_{76}(17490)$,¹⁸ $Gd_3N@C_{78}(22010)$,¹⁹ $Gd_3N@C_{82}(39663)$,²⁰ and $M_3N@C_{84}(51365)$ ($M = Gd$ and Tm).²¹⁻²² To the best of our knowledge, the latter is the largest non-IPR carbon cage characterized by X-ray. Also, two non-classical carbon networks containing a heptagon and thirteen pentagons have been stabilized by the presence of a metal cluster inside and characterized by X-ray, $LaSc_2N@C(\text{hept})-C_{80}$ ²³ and $Sc_2C_2@C(\text{hept})-C_{88}$.²⁴

A second way of violating the IPR rule emerged by exohedral derivatization with halogens. In the Kräschmer–Huffman arc discharge reactor non-IPR fullerenes can be more reactive than IPR ones because of the presence of fused pentagons. Although gas-phase experiments had shown that smaller non-IPR fullerene ions could be reduced and form hydrogenated adducts, it was in 2004 when a smaller fullerene, $C_{50}(271)$, was captured by chlorination and characterized by X-

ray. Since then, many other examples have been reported with this technique being $C_{78}(23863)Cl_8$, the largest non-IPR cage obtained.²⁵⁻²⁶ Beyond the formation of chlorinated fullerenes in an arc-discharge process in presence of additives, more classical chemical approaches have been used to synthesize halogen derivatives of C_{60} and other fullerenes. Important success has been achieved in preparation and characterization of fullerene bromides, fluorides and chlorides, with the formation in some case of highly halogenated species, such as $C_{60}Cl_{30}$,²⁷ $C_{60}F_{36}$ or $C_{60}F_{48}$.²⁸ The factors governing chlorination and other halogenations have been recently analyzed from topological models that incorporate the effects of π delocalization, cage strain, and steric hindrance.²⁹ Often, the carbon cage is strongly modified as the number of halogens increase. In particular, the reaction of $D_2-C_{76}(19150)$ with $SbCl_5$ affords the chlorinated $C_{76}Cl_{24}$ with a high number of fused pentagons.³⁰ In other cases, carbon cages containing heptagons are formed via C_2Cl_n loss.³¹⁻³² Chlorination followed by a single-crystal X-ray diffraction analysis has proved to be a powerful strategy to study giant fullerenes, which are available in the production soot in very small quantities.³³⁻³⁵ Theoretical³⁶⁻³⁷ and experimental studies³⁸ on chlorinated fullerenes have also shown to be very useful to understand the complex mechanism of fullerene formation.

In order to get a deeper knowledge on the bonding of Cl atoms on a fullerene surface, we have investigated by means of DFT calculations and Car-Parrinello molecular dynamics simulations the chlorination of the relatively simple non-IPR C_{72} . Among the 11190 possible isomers of C_{72} , only one with D_{6d} symmetry follows the IPR rule, which peculiarly³⁹ is higher in energy than the non-IPR isomer of C_{2v} symmetry and a Fowler-Monolopoulos code of 11188.⁴⁰ The energy difference between the two isomers is not small, as reported initially in a relatively old theoretical study⁴¹ and confirmed in more recent investigations.⁴² Isomer $C_{2v}(11188)$ has been synthesized and stabilized as $C_{72}Cl_4$ in the chlorine-involving carbon arc by two independent

teams.⁴³⁻⁴⁴ Here, we will try to understand the stability of the observed species, how they are formed and why the fullerene is captured as $C_{72}Cl_4$, whereas its partner with two additional carbon atoms has been characterized as $C_{74}Cl_{10}$.

2. Computational Details

All electronic structure calculations were performed using Density Functional Theory (DFT) methodology with the Amsterdam Density Functional code (ADF2013).⁴⁵⁻⁴⁶ The electronic density was provided by the local density approximation using Becke's gradient corrected exchange functional, and Vosko, Wilk, Nusair (VWN)⁴⁷ parametrization for correlation, corrected with Perdew's functional (BP86).⁴⁸ Triple- ζ polarization basis sets (TZP) were used to describe the electrons of the carbon and chlorine atoms. Scalar relativistic corrections were included by means of the zeroth-order regular approximation (ZORA) formalism. In addition, dispersion corrections by Grimme (D3) were included in our calculations.⁴⁹

Molecular dynamics simulations were performed by means of the Car-Parrinello Molecular Dynamics (CPMD) program.⁵⁰ The description of the electronic structure was based on the expansion of the valence electronic wave functions into a plane wave basis set, which was limited by an energy cutoff of 40 Ry. The interaction between the valence electrons and the ionic cores was treated through the pseudopotential (PP) approximation (Martins-Troullier type).⁵¹ The functional by Perdew, Burke, and Ernzerhoff (PBE) was selected as the density functional,⁵² and dispersion corrections (Grimme) were considered. We used a fictitious electron mass of 800 a.u. The Nosé-Hoover thermostat for the nuclear degrees of freedom was used to maintain the temperature as constant as possible. In all simulations, the wave function is converged at the beginning of the MD run. The simulations were carried out in a cubic cell with a side length of 15 Å and a time step of 0.144 fs. Periodic boundary conditions were used. A data set collection

of computational results is available in the ioChem-BD repository⁵³ and can be accessed via <https://doi.org/10.19061/iochem-bd-2-24>.

3. Results and Discussion

3.1. Stability of neutral cages

Since chlorination in the arc-reactor is found to take place once the neutral fullerenes are formed, we are first interested in discussing on the relative stabilities of neutral C_{72} cages.^{36, 38, 54} As already pointed out in previous studies⁴¹⁻⁴² and in our calculations compiled in Table 1, C_{72} fullerene family is rather unique because it does not fulfill the IPR rule. The APP1 cage #11188 with C_{2v} symmetry (Figure 1) is clearly more stable than the only IPR isomer with D_{6d} symmetry (around 15 kcal·mol⁻¹) and other APP1 and APP2 isomers (> 20 kcal·mol⁻¹). Taking into account that, in general, the penalty for each fused pentagon is about 18-20 kcal·mol⁻¹, the relative great stability of isomer #11188 is an anomaly in empty fullerenes. This circumstance can be easily rationalized from Figure 2, which shows that the classical IPR C_{70} and the APP1 cages C_{2v} - C_{72} (11188) and C_1 - C_{74} (14049) are linked by C_2 insertions. Therefore, the non-IPR cage C_{2v} - C_{72} (11188) can be seen as a result of a simple C_2 insertion into C_{70} , the second most stable fullerene after C_{60} . This point, together with the fact that the only C_{72} IPR isomer is topologically linked to an APP2 cage of C_{70} , explains the singular behavior observed for the C_{72} family. An analogous behavior was found for C_{62} , where the non-classical heptagon-containing C_{62} cage that results from single C_2 insertion on the iconic IPR C_{60} shows the lowest energy compared to classical non-IPR isomers.⁵⁵ Fullerene C_1 - C_{74} (14049), which has been also stabilized by chlorination and isolated and characterized as $C_{74}Cl_{10}$,³⁷ is linked to C_{2v} - C_{72} (11188) also by a simple

C_2 insertion. However, the relative energy of isomer C_1 - C_{74} (14049) with respect to the only IPR C_{74} isomer (14246) is 21.1 kcal·mol⁻¹. These two carbon cages are related by a single Stone-Wales transformation (SW) and therefore it is not unexpected the computed energy difference. Given that the most stable isomers for C_{70} , C_{80} , C_{90} , etc. can be seen as a C_{60} with 10, 20 or 30 C atoms inserted in the equatorial region of the cage one could speculate on the possibility of finding for C_{82} or C_{92} the same behavior observed for C_{72} ; however, for each of these cases, the topology is different and the C_2 insertion in the equatorial region would give a fullerene containing a heptagon (see Figure S2).

Table 1. Symmetries, Relative Energies and Free Energies for Selected Isomers of C_{72} .^{a)}

Isomer Number ^{b)}	Sym	Type ^{c)}	ΔE	ΔG (300 K)	ΔG (1000 K)
11190	D_{6d}	IPR	14.9	15.7	18.4
10612	C_2	APP1	23.8	22.4	21.1
11030	C_s	APP1	21.1	20.3	19.3
11188	C_{2v}	APP1	0.0	0.0	0.0
10538	C_1	APP2	23.5	22.4	21.1
10784	C_1	APP2	24.8	23.8	22.4

a) Energies are in kcal·mol⁻¹; b) Selected isomers in a range of 25 kcal·mol⁻¹; c) IPR: isolated pentagon rule; APPn: number of adjacent pentagon pairs

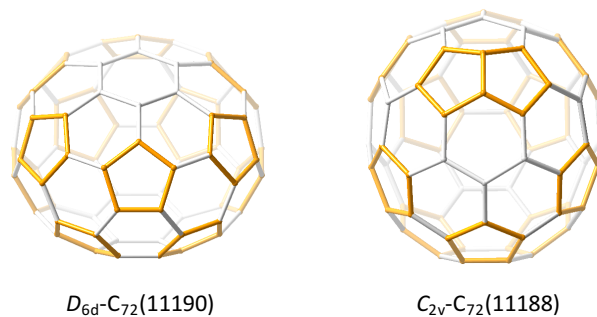


Figure 1. Molecular representation for non-IPR $C_{2v}\text{-}C_{72}(11188)$ and IPR $D_{6d}\text{-}C_{72}(11190)$ cages.

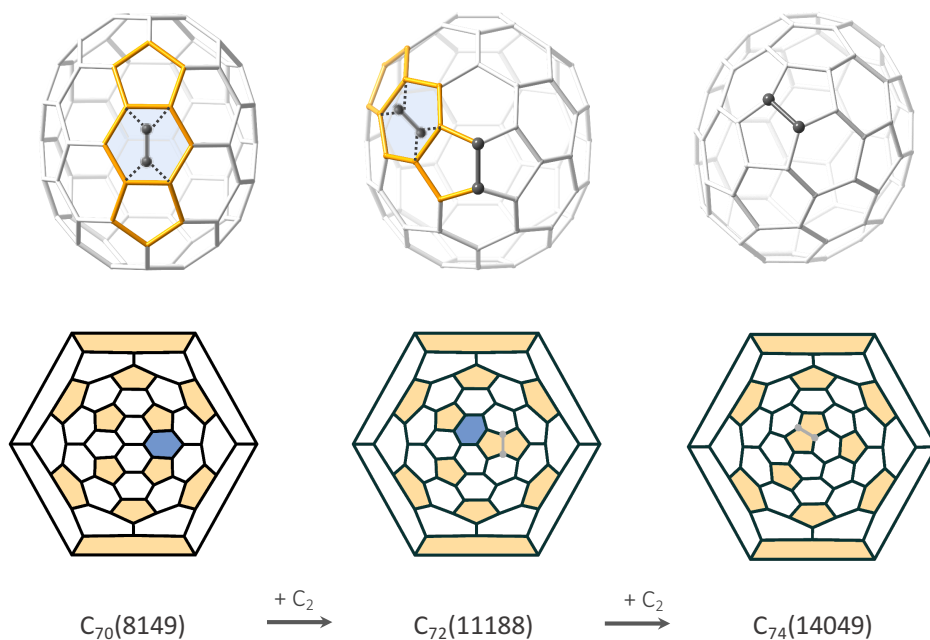


Figure 2. Schematic representation for the formal link between the IPR C_{70} and the non-IPR APP1 $C_{72}(11188)$ and $C_{74}(14049)$ fullerenes. The hexagons where the C_2 insertions must take place to transform $C_{70}(8149)$, first into $C_{72}(11188)$, and then into $C_{74}(14049)$ are highlighted in blue.

3.2. Formation of $C_{2v}\text{-}C_{72}(11188)\text{Cl}_4$: Stepwise radical addition

Single crystals of $C_{2v}\text{-}C_{72}(11188)\text{Cl}_4$, suitable for X-ray diffraction analysis were firstly reported separately by Xie *et al.* and Jansen *et al.* in two consecutive articles in the Journal of the American Chemical Society in 2010.^{43,44} The unfavorable local strain at the vertexes of the

pentagon fusion in C_{2v} - C_{72} (11188) can be released through bonding to two chlorine atoms. In addition to the two chlorine atoms associated with the pentagon fusion, other two chlorine atoms are bonded at two additional pentagon–hexagon–hexagon vertexes in a zigzag manner, as shown in Figure 3.

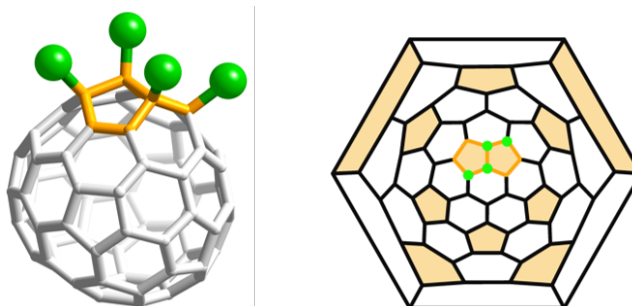


Figure 3. DFT-optimized structure and Schlegel diagram for the C_{2v} - C_{72} (11188)- Cl_4 structure. Chlorine atoms represented as green balls; pentagons highlighted in orange.

Even though C_{2v} - C_{72} (11188) is predicted to have a lower energy than the IPR D_{6d} - C_{72} (11190), it has never been observed as pristine empty fullerene remaining as one of the missing fullerenes so far. The HOMO-LUMO gap, which is related to the kinetic stability of the molecule, increases significantly upon chlorination from 0.65 eV in the pristine cage to 1.24 eV in the tetrachloride as shown in Table 2 (at BP86/TZP level, to be compared with 1.66 eV for C_{60}).

As observed for other chlorofullerenes,^{37,38} the radical addition to a fullerene can be understood from the atomic orbital contributions to the HOMO and the spin density distribution for those cages with an odd number of Cl atoms. The shapes of the HOMOs for the closed-shell systems C_{2v} - C_{72} (11188) and C_{2v} - C_{72} (11188) Cl_2 together with the spin density for the radical C_{2v} - C_{72} (11188) Cl_3 are shown in Figure 4 along with the stepwise chlorination pathway. The first two chlorine atoms are added sequentially to the pentalene bond of the fused pentagons so that strain is maximally

released. The C atoms in these pentalene bonds are by far the two most pyramidalized atoms in the structure (pyramidalization angles of 16.6°). In addition, these two atoms show the highest atomic orbital contributions to the HOMO of C_{72} (see Figure 4). Once the first chlorine was added in any of the two C atoms of the pentalene bond, the two possible $C_{72}Cl$ radicals that could be generated show significant values of the spin density on the other C atom of the pentalene. However, some other neighboring C atoms are found to show larger spin densities (see Figure S3). Chlorination in one of these neighboring C atoms leads to regioisomers with higher energies (around 10 kcal mol⁻¹) compared to that for dichlorination on the pentalene. Therefore, it seems that release of strain due to bonding to the pentalene is the trend-setting factor for the second chlorination step. On the basis of the highest contribution to the HOMO of $C_{72}Cl_2$, the next position to be chlorinated is one [5, 6, 6] C atom contiguous to the pentalene bond, indicated by an arrow in $C_{72}Cl_2$ or as a black dot in the Schlegel diagram in Figure 4. For the $C_{72}Cl_3$ radical, the next chlorination position was found to be that with the four chlorine atoms placed in the fused pentagons in a zigzag manner (see Figure 4).

Binding energies (BE) between the C_{2v} - C_{72} (11188) cage and chlorine atoms have been analysed to predict quantitatively the stability of the external atoms bonding to the empty cage (Tables S1, S2, S3 and S4). The C-Cl binding energy per chlorine atom, BE_{C-Cl} , was calculated by equation [1], where 'x' represents the number of chlorine atoms.

$$BE_{C-Cl} = [E(C_{72}Cl_x) - E(C_{72}) - x E(Cl)]/x \quad [1]$$

These binding energies in C_{2v} - C_{72} (11188) were found to be similar as in other chlorinated fullerenes detected so far (ca. -50 kcal·mol⁻¹).³⁶⁻³⁸ The binding energies for the first and second chlorines, which attach to the pentalene bond, are ca. -60 kcal·mol⁻¹. We checked that the binding energies for chlorination and dichlorination at other positions of the cage are much

lower. The reactivity in the pentalene is much more important than in other positions of the fullerene surface, where the pyramidalization of the carbon atoms is less important. The C–Cl binding energies for radicals $C_{2v}\text{-}C_{72}(11188)\text{Cl}_x$ ($x = 1$ and 3) are significantly smaller than those for closed-shell species ($x = 2, 4$). The binding energy for $x = 4$ is rather high ($-53 \text{ kcal}\cdot\text{mol}^{-1}$), but the energy for the addition of the second chlorine is by far the largest one ($-60 \text{ kcal}\cdot\text{mol}^{-1}$), once the strain in the pentalene bond is released. Consequently, we infer that the dichlorinated cage $C_{72}\text{Cl}_2$ might be formed under slightly different experimental conditions at lower chlorine concentration. We have also computed the C-Cl bond free energies for some carbon atoms (#6 and #7) and observed analogous relative energies with somewhat less negative (more positive) absolute values due mainly to the negative translational entropic term (see SI).

Table 2. C-Cl Binding Energies and HOMO-LUMO Gaps for $C_{2v}\text{-}C_{72}(11188)\text{Cl}_x$ ($x = 0\text{-}4$) at Different Stages of Chlorination.

System	BE_{c-cl}	H-L gap
C_{72}		0.65
$C_{72}\text{Cl}_1$	-45.3	
$C_{72}\text{Cl}_2$	-59.5	0.70
$C_{72}\text{Cl}_3$	-42.3	
$C_{72}\text{Cl}_4$	-53.4	1.24

a) BE_{c-cl} in kcal·mol⁻¹ and H-L gaps in eV; b) H-L gaps only for closed-shell systems.

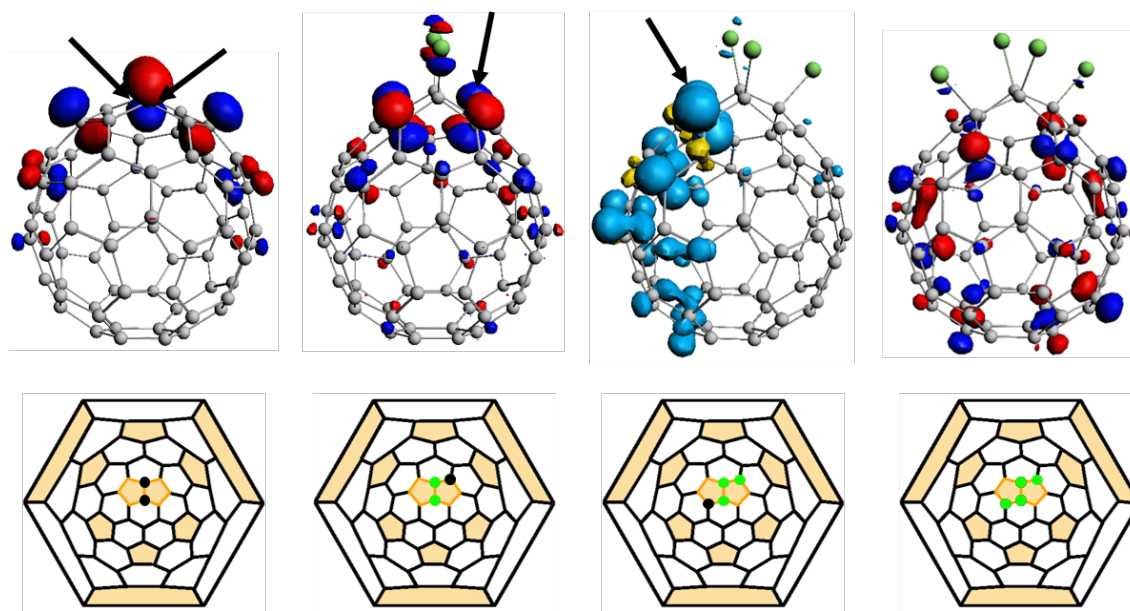


Figure 4. Representation of the HOMO (for C_{72} , $C_{72}Cl_2$ and $C_{72}Cl_4$) and the spin density (for $C_{72}Cl_3$) distributions, along with the corresponding Schlegel diagrams, for different steps of the chlorination pathway. The green dots in the Schlegel diagrams indicate the positions of the chlorine atoms. The black arrows in the three-dimensional structure and the black dots in the Schlegel diagrams show the position where the next chlorine atom is added.

3.3. Formation of C_{2v} - $C_{72}(11188)Cl_4$: Insights on the dynamical process

Car-Parrinello Molecular Dynamics simulations were performed to provide more insight into the motion of chlorines in C_{2v} - $C_{72}(11188)Cl_4$ at different temperatures (1000, 1300, 1400 and 1500 K). Trajectories at 1400 and 1500 K for C_{2v} - $C_{72}(11188)Cl_4$ show that chlorine atoms are lost after the first 7 and 3 ps, respectively (Figure 5). Those chlorine atoms attached to the pentalene bond are lost at longer simulation times. In contrast, trajectories at 1000 and 1300 K show that the four chlorines remain in their original positions at the rather short time scale simulated here (around 30 ps), as shown in Figure 5. These results for C_{2v} - $C_{72}(11188)$ confirm the already proposed mechanism for the formation of chlorofullerenes in the arc, which considers that initially the

carbon cage is formed at high temperatures and then, further from the arc center and at lower temperatures, chlorination takes place.^{38,43}

To have more understanding into the chlorination of the C_{2v} - C_{72} (11188) fullerene, another set of Car-Parrinello MD simulations were run with different initial conditions (initial temperatures and densities of Cl atoms). For example, Figure 6 shows six representations along the trajectory of the system composed by C_{2v} - C_{72} (11188) and 4 Cl atoms; more snapshots are shown in Figure S4. The temperature is decreased along the simulation, starting from 800 K down to 350 K. At the beginning of this trajectory, chlorine atoms are attached to the pentalene bond and in other positions of the fullerene surface (fourth snapshot in Figure 6, at 40 ps). Migration of chlorine atoms is also observed along the trajectory (second and third snapshot in Figure 6), as well as the attachment of Cl atoms on the cage and their subsequent detachment. When temperature decreases to at least 500 K, two chlorine atoms keep attached to the pentalene bond, which shows the largest pyramidalization angles and C-Cl binding energies. Initial geometries of chlorines are not so relevant because Cl atoms can easily collide, bond or migrate on the fullerene surface to find a more stable structure during the simulation. Interestingly, in all the trajectories, we observe (i) formation of C-Cl bonds in the most favored carbon positions, i.e. in the pentalene bond; (ii) formation and breaking of C-Cl bonds in less favored positions; and (iii) migration ability of Cl atoms on the carbon surface. However, we have not observed the formation of the experimental C_{2v} - C_{72} (11188)Cl₄ molecule in the short time scale of our simulations (130 ps). From these results, we infer that chlorination of carbon cages might take place according to the following considerations: (i) Cl atoms bond to the fullerene in non-specific positions; (ii) if the temperature is high enough to break the C-Cl bonds, the bonds are broken; (iii) when the Cl atoms bond to the most favored positions of the cage, as for example to

the pentalene, the C-Cl bond is stronger and as the temperature decreases they are trapped in these positions; (iv) when the Cl atoms attach to other non so-favored positions, they can migrate on the surface to reach the most favored ones from a thermodynamic point of view.

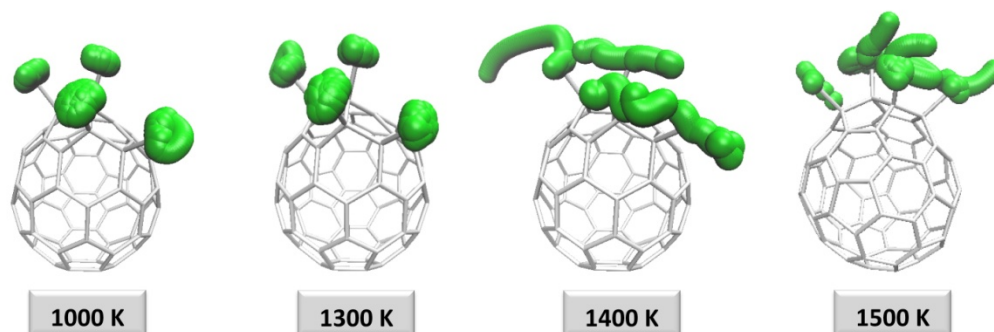


Figure 5. Representation of the motion of chlorine atoms in the $C_{2v}-C_{72}(11188)Cl$ structure during the Car-Parrinello MD simulations at different temperatures (1000 K, 1300 K, 1400 K and 1500 K).

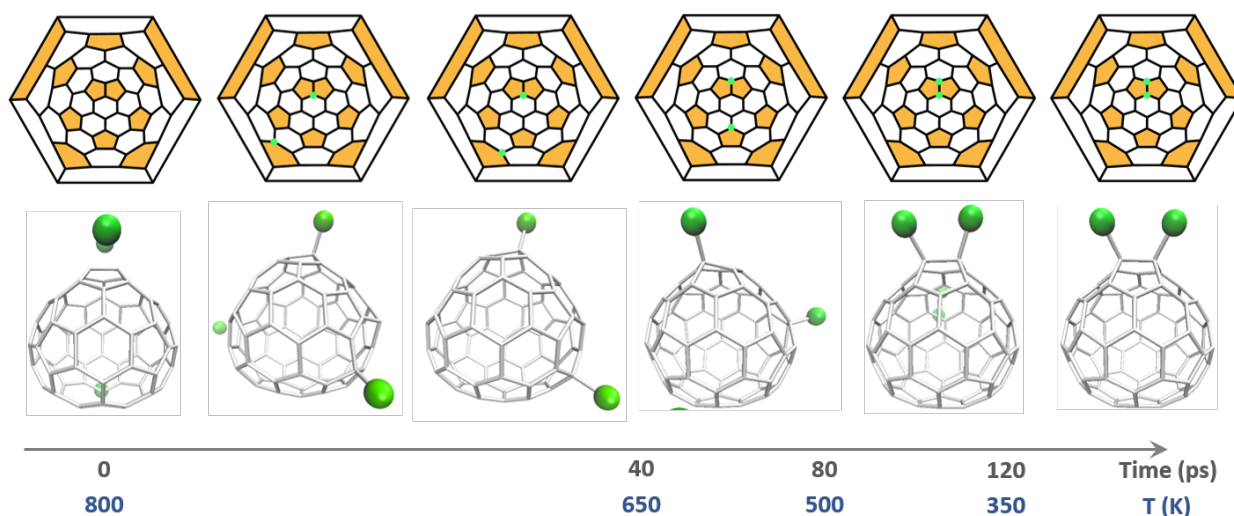


Figure 6. Snapshots of the Car-Parrinello MD simulation of $C_{2v}-C_{72}(11188)$ and 4 Cl atoms during 130 ps and decreasing the temperature from 800 down to 350 K.

snapshot are also shown, which represent the chlorine atoms (green dots) that are attached on the surface cage.

3.4. Migration of chlorines on the fullerene surface

To give support to the proposed mechanism for chlorination, we have investigated in detail the energetics of the likely migration of chlorine atoms on the fullerene surface observed in Car-Parrinello simulations. We have carried out a comprehensive study of the migration barriers of Cl between two C positions at different levels of chlorination ($x = 1$ up to 4). The barriers can range from very small values around 0-1 kcal·mol⁻¹ to larger values around 25 kcal·mol⁻¹ (see Table 3). Therefore, migrations of Cl atoms are attainable at chlorination temperatures and they can even be very fast processes as observed in standard Car-Parrinello simulations.

In particular, we have analyzed the migrations around the pentalene motif, which are the positions that lead to the most favored chlorinated regioisomers. For $x=1$, the electronic barriers range from 1 to 18 kcal·mol⁻¹. The largest one, 17.6 kcal·mol⁻¹, corresponds to the migration between the two C atoms of the pentalene bond (1 → 2), which are the two lowest-energy degenerate monochlorinated regioisomers. The lowest barrier, ~1 kcal·mol⁻¹, corresponds to the 22 → 7 migration, in line with the low stability of the initial regioisomer (22). Migration to a C atom of the pentalene (6 → 1), which is thermodynamically favoured by 9.6 kcal·mol⁻¹, shows a barrier of only 10.3 kcal·mol⁻¹. Once position 2 is chlorinated, for $x=2$, we found a very low barrier of 1.5 kcal·mol⁻¹ and a barrierless process that correlates with a two rather favorable migrations (19 → 6 and 22 → 7, respectively). Interestingly, the barrier for migration from 7 to 6 (8.7 kcal·mol⁻¹) is somewhat reduced compared to $x=1$, in line with the stabilization of the final dichlorinated product on position 6, one of the C atoms with the largest spin densities in C_{2v} -

$C_{72}(11188)Cl$ (*vide supra*). In contrast, the barrier for the $6 \rightarrow 1$ migration is slightly enhanced ($14.6 \text{ kcal}\cdot\text{mol}^{-1}$) compared to $x=1$. Once the pentalene bond is chlorinated, for $x=3$, we again found that the barrier for the $19 \rightarrow 6$ migration is very low ($1.5 \text{ kcal}\cdot\text{mol}^{-1}$), as well as that for $22 \rightarrow 7$ process ($0.6 \text{ kcal}\cdot\text{mol}^{-1}$). Now, the $7 \rightarrow 6$ migration is significantly favoured from a thermodynamic point of view, i.e. it leads to one of the lowest-energy $C_{2v}-C_{72}(11188)Cl_3$ regioisomers (*vide supra*), and the barrier is also very low ($2.6 \text{ kcal}\cdot\text{mol}^{-1}$). Migration from 20 to 19 showed the highest computed barrier ($19.0 \text{ kcal}\cdot\text{mol}^{-1}$), in line with the process being quite unfavorable ($17.9 \text{ kcal}\cdot\text{mol}^{-1}$). When the $C_{2v}-C_{72}(11188)Cl_3$ radical is formed, many of the computed barriers are rather low (below $4 \text{ kcal}\cdot\text{mol}^{-1}$), in particular those for the most exothermic processes (chlorination on position 6). We found at this point the highest barrier from all those computed here, which corresponds to the highly unfavorable $20 \rightarrow 19$ migration ($24.4 \text{ kcal}\cdot\text{mol}^{-1}$). We have checked for some of the migrations that the reaction free energies and barriers are kept essentially unchanged (see SI).

Table 3. Relative Energies for the Final Regioisomers and Transition States with Respect to the Initial Regioisomers for Chlorine Migration Processes on the Fullerene $C_{2v}\text{-}C_{72}(11188)Cl_x$.^a

x	Migration	Barriers	Final
1	21 → 22	14.4	14.3
	22 → 7	~1 ^b	-19.6
	7 → 6	12.8	3.6
	6 → 1	10.3	-9.6
	1 → 2	17.6	0.0
2	19 → 6	1.5	-17.4
	22 → 7	0.0	-15.6
	21 → 22	~9 ^c	8.3
	7 → 6	8.7	-6.9
	6 → 1	14.6	-9.7
3	21 → 20	6.7	-8.0
	20 → 19	19.0	17.9
	19 → 6	1.5	-22.8
	21 → 22	11.7	11.7
	22 → 7	0.6	-5.0
4	7 → 6	2.6	-19.6
	21 → 20	3.9	-14.3
	20 → 19	24.4	23.6
	19 → 6	0.4	-31.6
	21 → 22	11.0	8.8
	22 → 7	1.1	-7.2
	7 → 6	3.9	-23.9

^a Energies in kcal·mol⁻¹; ^b We have not been able to find this TS; we estimate the barrier to be around 1 kcal mol⁻¹ comparing with the TS for the same migration for x = 2, 3 and 4. ^c We have not been able to find this TS; we estimate the barrier to be around 9 kcal mol⁻¹ comparing with the TS for the same migration for x = 1, 3 and 4, for which the energy is very similar to the energy of the final regioisomer (22).

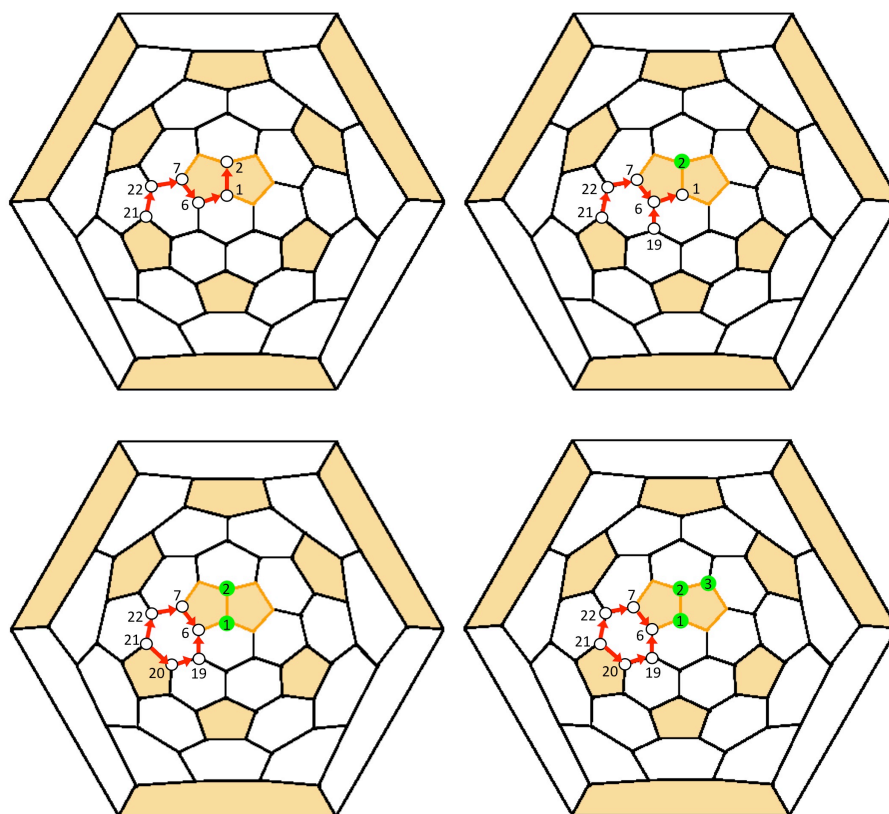


Figure 7. Schlegel diagrams showing the pathways considered for the migration of Cl atoms on the fullerene surface for C_{2v} - $C_{72}(11188)Cl_x$, where $x=1, 2, 3, 4$.

3.5. Can we predict the level of chlorination? $C_{72}Cl_4$ vs $C_{74}Cl_{10}$

The introduction of chlorine atoms effectively reduces reactive sites of pristine cages, improving the solubility and preventing from polymerization. However, some of the questions that we might wonder at this point are 'Why is cage C_{2v} - $C_{72}(11188)$ experimentally formed with four and not with other number of Cl atoms?', 'Could it be possible to find the same cage with a

different number of chlorines?' or 'Why does $C_{2v}-C_{72}(11188)$ take four chlorines and $C_1-C_{74}(14049)$ takes instead ten of them?'. With the aim of trying to answer these questions, we computed the binding energies for $C_{2v}-C_{72}(11188)Cl_x$ ($x = 5-10$) to compare them with those for $C_1-C_{74}(14049)Cl_x$ ($x = 5-10$) and also performed Car-Parrinello MD simulations on $C_{2v}-C_{72}Cl_5(11188)$.

Binding energies for chlorination of $C_{2v}-C_{72}(11188)Cl_x$ and $C_1-C_{74}(14049)Cl_x$ ($x = 1-10$) are shown in Figure 8 and Tables S6-11. The chlorination pattern for $C_{2v}-C_{72}(11188)Cl_x$ ($x = 5-10$) is based on the empirical rules derived previously.³⁶ The energies released when attaching two chlorines to the pentalene bond are quite similar for $C_{2v}-C_{72}(11188)$ and $C_1-C_{74}(14049)$, being the latter slightly favored by around 5 kcal mol⁻¹. The energies for the binding of the third chlorine are also quite similar between them, but smaller than for the first two steps. The fourth chlorination is very favored for $C_{2v}-C_{72}(11188)$ (-53.4 kcal·mol⁻¹), while the binding energy for $C_1-C_{74}(14049)Cl_4$ is significantly smaller (-46.4 kcal·mol⁻¹). This important binding energy difference makes us think that $C_{2v}-C_{72}(11188)$ is a rather stable cage with four Cl in the pentalene motif, which is in line with its experimental isolation and characterization. Interestingly, the energy released for the first four steps is essentially the same for the two cages. Thus, according to this very simple criterion, $C_1-C_{74}(14049)Cl_4$ should be is also expected to be observed. As shown in Figure 8, the binding energies for the next radical species ($x = 5, 7, 9$) are significantly smaller than those for closed-shell species ($x = 6, 8, 10$), particularly for $C_{2v}-C_{72}(11188)$ cage. The binding energy for $x = 10$ is by far the largest one for $C_1-C_{74}(14049)$ (-64.9 kcal·mol⁻¹), which should be related to the fact that it has been also isolated and characterized. We checked that binding energies for chlorination at other positions of the $C_{2v}-C_{72}(11188)$ cage are much lower (see SI). Finally, the energy released for the ten chlorination steps is by far larger (34 kcal mol⁻¹) for $C_1-C_{74}(14049)$ than for $C_{2v}-C_{72}(11188)$, which might be related to the

impossibility of closing the belt of chlorines on the surface as a consequence of the 1,4-additions³⁶ and explain why $C_{2v}\text{-}C_{72}(11188)\text{Cl}_{10}$ has not been obtained so far.

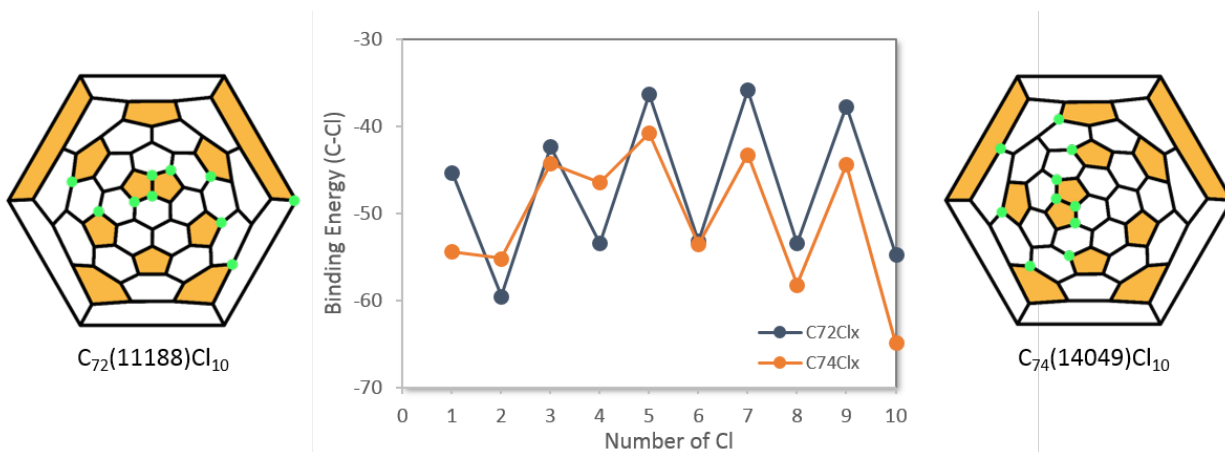


Figure 8. C-Cl binding energies (BE_{c-cl}) at different stages of chlorination for $C_{2v}\text{-}C_{72}(11188)\text{Cl}_x$ and $C_1\text{-}C_{74}(14049)\text{Cl}_x$ ($x = 0\text{-}10$), and their Schlegel diagrams with 10 chlorines.

Car-Parrinello MD simulations on three different regioisomers of the hypothetical $C_{2v}\text{-}C_{72}(11188)\text{Cl}_5$ molecule have been done at different temperatures in order to gain more insight into the behavior of an extra chlorine on the surface of $C_{2v}\text{-}C_{72}(11188)\text{Cl}_4$ (Figure 9). In all trajectories, run at different temperatures (200, 300, 400, 500, 600, 800, and 1000 K), the four chlorines attached to the pentalene remained in their original positions without leaving the fullerene at any moment at the time scale of our simulations (30 ps). However, the fifth chlorine is observed to migrate on the cage surface in a rather easy manner and/or detach from the cage in most of the trajectories at rather low temperatures (Figure 9). The free energy barriers associated to the migration of the fifth chlorine are rather attainable at the simulated temperatures, i.e. a) 1.2, b) 13.7 and c) 8.9 kcal·mol⁻¹ in Figure 9, for the three different positions considered here, in

agreement with the barriers found at lower levels of chlorination (*vide supra*). We also observed that the extra chlorine atom quickly detaches from the C_{2v} - C_{72} (11188) cage at temperatures higher than 800 K. These results corroborate the enhanced stability of the formed product C_{2v} - C_{72} (11188)Cl₄.

To end up, even though we are not able to provide definite answers to those specific questions formulated at the beginning of this paragraph, the binding energies and the Car-Parrinello simulations provide us with some hints that help to rationalize the experimental results.

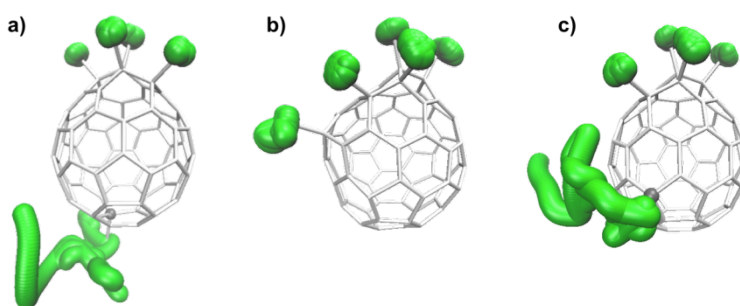


Figure 9. Representation of the motions of chlorines for three different regioisomers of C_{2v} - C_{72} (11188)Cl₅ at 800 K.

Conclusions

The fullerene with 72 carbon atoms presents the singularity that the only IPR isomer of symmetry D_{6d} is not the most stable empty cage, but the non-IPR isomer C_{2v} - C_{72} (11188), which is about 15 kcal·mol⁻¹ lower in energy. This anomaly occurs because the non-IPR cage is linked to the very stable IPR isomer of C_{70} by a simple C_2 insertion, whereas isomer D_{6d} is topologically linked to an APP2 isomer of C_{70} . In non-IPR cages, the carbon atoms belonging to the fused pentagons are more reactive against halogens and hydrogen atoms. In this context, fullerene C_{2v} - C_{72} (11188) was synthesized in a Kräschmer–Huffman arc discharge apparatus as C_{72} Cl₄. DFT

calculations and Car-Parrinello molecular dynamics simulations have allowed us to rationalize how chlorine atoms are trapped in the fullerene surface, as well as their mobility over the surface providing hints about the chlorination mechanism once the fullerene cages have been formed. For carbon atoms that exhibit relatively small C-Cl binding energies, chlorine migration to neighboring sites, were observed in molecular dynamics trajectories, in line with their computed low free energy barriers.

We have also given more insight on why C_{74} has been captured as $C_{74}Cl_{10}$, while on the surface of C_{72} only four Cl atoms were trapped. Despite $C_{74}(14049)$ links to $C_{2v}-C_{72}(11188)$ also by a simple C_2 insertion the topology of two cages is somewhat different, thus exhibiting different reactivity.

Acknowledgments

This work was supported by the Spanish Ministerio de Ciencia e Innovación (Project No. CTQ2017-87269-P) and by the Generalitat de Catalunya (2017SGR629 and XRQTC). J.M.P. thanks the ICREA foundation for an ICREA ACADEMIA award. L.A. thanks the Generalitat de Catalunya for a predoctoral fellowship (FI-DGR 2014).

Supporting Information

The Supporting Information is available free of charge on the ACS Publications website at DOI: .

Schlegel diagram for $C_{2v}-C_{72}(11188)$ cage, spin density for $C_{2v}-C_{72}(11188)Cl$, snapshots of the Car-Parrinello MD simulation of $C_{2v}-C_{72}(11188)$ and 4 Cl during 130 ps, C-Cl binding energies for $C_{2v}-C_{72}(11188)Cl_x$ and $C_1-C_{74}(14049)Cl_x$, binding free energies and migration free energy

barriers for $C_{2x}-C_{7x}(11188)Cl_x$ and xyz coordinates of the lowest-energy $C_{2x}-C_{7x}(11188)Cl_x$ isomers ($x = 1$ to 4).

References

1. Kroto, H. W.; Heath, J. R.; O'Brien, S. C.; Curl, R. F.; Smalley, R. E., C60: Buckminsterfullerene. *Nature*, **1985**, *318*, 162-163.
2. Dresselhaus, M. S.; Dresselhaus, G.; Eklund, P. C., *Science of Fullerenes and Carbon Nanotubes*. USA, 1996.
3. Sharma, R.; Kar, K. K., *Carbon Nanotubes: Synthesis, Characterization and Applications*. 2011.
4. Kroto, H. W., The Stability of the Fullerenes C_n , with $n = 24, 28, 32, 36, 50, 60$ and 70 . *Nature*, **1987**, *329*, 529-531.
5. Wang, C. R.; Kai, T.; Tomiyama, T.; Yoshida, T.; Kobayashi, Y.; Nishibori, E.; Takata, M.; Sakata, M.; Shinohara, H., Materials Science: C_{60} Fullerene Encaging a Scandium Dimer. *Nature*, **2000**, *408*, 426-427.
6. Stevenson, S.; Fowler, P. W.; Heine, T.; Duchamp, J. C.; Rice, G.; Glass, T.; Harich, K.; Hajdu, E.; Bible, R.; Dorn, H. C., Materials Science: A Stable Non-Classical Metallofullerene Family. *Nature*, **2000**, *408*, 427-428.
7. Rodríguez-Fortea, A.; Alegret, N.; Balch, A. L.; Poblet, J. M., The Maximum Pentagon Separation Rule Provides a Guideline for the Structures of Endohedral Metallofullerenes. *Nature Chem.*, **2010**, *2*, 955–961.

8. Rodríguez-Forteza, A.; Balch, A. L.; Poblet, J. M., Endohedral Metallofullerenes: A Unique Host-Guest Association. *Chem. Soc. Rev.*, **2011**, *40*, 3551-3563.
9. Shi, Z. Q.; Wu, X.; Wang, C. R.; Lu, X.; Shinohara, H., Isolation and Characterization of $\text{Sc}_2\text{C}_2@C_{68}$: A Metal-Carbide Endofullerene with a Non-IPR Carbon Cage. *Angew. Chem. Int. Ed.*, **2006**, *45*, 2107-2111.
10. Yang, S. F.; Popov, A. A.; Dunsch, L., Violating the Isolated Pentagon Rule (IPR): the Endohedral Non-IPR C_{70} Cage of $\text{Sc}_2\text{N}@C_{70}$. *Angew. Chem. Int. Ed.*, **2007**, *46*, 1256-1259.
11. Chen, N.; Mulet-Gas, M.; Li, Y. Y.; Stene, R. E.; Atherton, C. W.; Rodríguez-Forteza, A.; Poblet, J. M.; Echegoyen, L., $\text{Sc}_3\text{S}@C_2(7892)-C_{70}$: A Metallic Sulfide Cluster Inside a Non-IPR C_{70} Cage. *Chem. Sci.*, **2013**, *4*, 180-186.
12. Feng, L.; Zhang, M.; Hao, Y.; Tang, Q.; Chen, N.; Slanina, Z.; Uhlířek, F., Endohedrally Stabilized C_{70} Isomer with Fused Pentagons Characterized by Crystallography. *Dalton Trans.*, **2016**, *45*, 8142-8148
13. Chen, N.; Beavers, C. M.; Mulet-Gas, M.; Rodríguez-Forteza, A.; Munoz, E. J.; Li, Y. Y.; Olmstead, M. M.; Balch, A. L.; Poblet, J. M.; Echegoyen, L., $\text{Sc}_2\text{S}@C(10528)-C_{70}$: A Dimetallic Sulfide Endohedral Fullerene with a Non Isolated Pentagon Rule Cage. *J. Am. Chem. Soc.*, **2012**, *134*, 7851-7860.
14. Wakahara, T.; Nikawa, H.; Kikuchi, T.; Nakahodo, T.; Rahman, G. M. A.; Tsuchiya, T.; Maeda, Y.; Akasaka, T.; Yoza, K.; Horn, E.; Yamamoto, K.; Mizorogi, N.; Slanina, Z.; Nagase, S., $\text{La}@C_{72}$ Having a Non-IPR Carbon Cage. *J. Am. Chem. Soc.*, **2006**, *128*, 14228-14229.

15. Kato, H.; Taninaka, A.; Sugai, T.; Shinohara, H., Structure of a Missing-Caged Metallofullerene: $\text{La}_2@C_{72}$. *J. Am. Chem. Soc.*, **2003**, *125*, 7782-7783.
16. Slanina, Z.; Chen, Z.; Schleyer, P. v. R.; Uhlík, F.; Lu, X.; Nagase, S., $\text{La}_2@C_{72}$ and $\text{Sc}_2@C_{72}$: Computational Characterizations. *J. Phys. Chem. A*, **2006**, *110*, 2231–2234.
17. Lu, X.; Nikawa, H.; Nakahodo, T.; Tsuchiya, T.; Ishitsuka, M. O.; Maeda, Y.; Akasaka, T.; Toki, M.; Sawa, H.; Slanina, Z.; Mizorogi, N.; Nagase, S., Chemical Understanding of a Non-IPR Metallofullerene: Stabilization of Encaged Metals on Fused-Pentagon Bonds in $\text{La}_2@C_{72}$. *J. Am. Chem. Soc.*, **2008**, *130*, 9129-9136.
18. Yang, S.; Popov, A. A.; Dunsch, L., The Role of an Asymmetric Nitride Cluster on a Fullerene Cage: The Non-IPR Endohedral $\text{DySc}_2\text{N}@C_{76}$. *J. Phys. Chem. B*, **2007**, *111*, 13659–13663.
19. Beavers, C. M.; Chaur, M. N.; Olmstead, M. M.; Echegoyen, L.; Balch, A. L., Large Metal Ions in a Relatively Small Fullerene Cage: The Structure of $\text{Gd}_3\text{N}@C_3(22010)-C_{78}$ Departs from the Isolated Pentagon Rule. *J. Am. Chem. Soc.*, **2009**, *131*, 11519-11524.
20. Mercado, B. Q.; Beavers, C. M.; Olmstead, M. M.; Chaur, M. N.; Walker, K.; Holloway, B. C.; Echegoyen, L.; Balch, A. L., Is the Isolated Pentagon Rule Merely a Suggestion for Endohedral Fullerenes? The Structure of a Second Egg-Shaped Endohedral Fullerene $\text{Gd}_3\text{N}@C_3(39663)-C_{82}$. *J. Am. Chem. Soc.*, **2008**, *130*, 7854–7855.
21. Beavers, C. M.; Zuo, T.; Duchamp, J. C.; Harich, K.; Dorn, H. C.; Olmstead, M. M.; Balch, A. L., $\text{Tb}_3\text{N}@C_{84}$: An Improbable, Egg-Shaped Endohedral Fullerene that Violates the Isolated Pentagon Rule. *J. Am. Chem. Soc.*, **2006**, *128*, 11352–11353.

22. Zuo, T.; Walker, K.; Olmstead, M. M.; Melin, F.; Holloway, B. C.; Echegoyen, L.; Dorn, H. C.; Chaur, M. N.; Chancellor, C. J.; Beavers, C. M.; Balch, A. L.; Athans, A. J., New Egg-Shaped Fullerenes: Non-Isolated Pentagon Structures of $Tm_3N@C_3(51365)-C_{84}$ and $Gd_3N@C_3(51365)-C_{84}$. *Chem. Commun.*, **2008**, 1067-1069
23. Zhang, Y.; Ghiassi, K. B.; Deng, Q.; Samoylova, N. A.; Olmstead, M. M.; Balch, A. L.; Popov, A. A., Synthesis and Structure of $LaSc_2N@Cs(\text{hept})-C_{80}$ with One Heptagon and Thirteen Pentagons. *Angew. Chem. Int. Ed.*, **2015**, *54*, 495-499.
24. Chen, C. H.; Abella, L.; Ceron, M. R.; Guerrero-Ayala, M. A.; Rodríguez-Forteza, A.; Olmstead, M. M.; Powers, X. B.; Balch, A. L.; Poblet, J. M.; Echegoyen, L., Zigzag Sc_2C_2 Carbide Cluster inside a 88 Fullerene Cage with One Heptagon, $Sc_2C_2@C(\text{hept})-C_{88}$: A Kinetically Trapped Fullerene Formed by C_2 Insertion? *J. Am. Chem. Soc.*, **2016**, *138*, 13030-13037.
25. Tan, Y. Z.; Xie, S. Y.; Huang, R. B.; Zheng, L. S., The Stabilization of Fused-Pentagon fullerene Molecules. *Nat. Chem.*, **2009**, *1*, 450-460.
26. Tan, Y. Z.; Li, J.; Zhou, T.; Feng, Y. Q.; Lin, S. C.; Lu, X.; Zhan, Z. P.; Xie, S. Y.; Huang, R. B.; Zheng, L. S., Pentagon-Fused Hollow Fullerene in C_{78} Family Retrieved by Chlorination. *J. Am. Chem. Soc.*, **2010**, *132*, 12648-12652.
27. Troshin, P. A.; Lyubovskaya, R. N.; Ioffe, I. N.; Shustova, N. B.; Kemnitz, E.; Troyanov, S. I., Synthesis and Structure of the Highly Chlorinated [60]Fullerene $C_{60}Cl_{30}$ with a Drum-Shaped Carbon Cage. *Angew. Chem. Int. Ed.*, **2005**, *44*, 234-237.

28. Kawasaki, S.; Aketa, T.; Touhara, H.; Okino, F.; Boltalina, O. V.; Gol'dt, I. V.; Troyanov, S. I.; Taylor, R., Crystal Structures of the Fluorinated Fullerenes $C_{60}F_{36}$ and $C_{60}F_{48}$. *J. Phys. Chem. B*, **1999**, *103*, 1223-1225.
29. Wang, Y.; Díaz-Tendero, S.; Alcamí, M.; Martín, F., Relative Stability of Empty Exohedral Fullerenes: π Delocalization versus Strain and Steric Hindrance. *J. Am. Chem. Soc.*, **2017**, 1609–1617.
30. Ioffe, I. N.; Goryunkov, A. A.; Tamm, N. B.; Sidorov, L. N.; Kemnitz, E.; Troyanov, S. I., Fusing Pentagons in a Fullerene Cage by Chlorination: IPR D_2 - C_{76} Rearranges into non-IPR $C_{76}Cl_{24}$. *Angew. Chem. Int. Ed.*, **2009**, *48*, 5904-5907.
31. Ioffe, I. N.; Mazaleva, O. N.; Sidorov, L. N.; Yang, S.; Wei, T.; Kemnitz, E.; Troyanov, S. I., Cage Shrinkage of Fullerene via a C_2 Loss: from IPR $C_{90}(28)Cl_{24}$ to Nonclassical, Heptagon-Containing $C_{88}Cl_{22/24}$. *Inorg. Chem.*, **2013**, *52*, 13821–13823.
32. Ioffe, I. N.; Chen, C.; Yang, S.; Sidorov, L. N.; Kemnitz, E.; Troyanov, S. I.; , Chlorination of C_{86} to $C_{84}Cl_{32}$ with Nonclassical Heptagon-Containing Fullerene Cage Formed by Cage Shrinkage. *Angew. Chem. Int. Ed.*, **2010**, *49*, 4784–4787.
33. Yang, S.; Wei, T.; Kemnitz, E.; Troyanov, S. I., First Isomers of Pristine C_{104} Fullerene Structurally Confirmed as Chlorides, $C_{104}(258)Cl_{16}$ and $C_{104}(812)Cl_{24}$. *Chem. Asian J.*, **2014**, *9*, 79–82.
34. Yang, S.; Wei, T.; Wang, S.; Ignat'eva, D. V.; Kemnitz, E.; Troyanov, S. I., The First Structural Confirmation of a C_{102} Fullerene as $C_{102}Cl_{20}$ Containing a Non-IPR Carbon Cage. *Chem. Commun.*, **2013**, *49*, 7944-7946.

35. Yang, S. F.; Wang, S.; Kemnitz, E.; Troyanov, S. I., Chlorination of IPR C_{100} Fullerene Affords Unconventional $C_{96}C_{20}$ with a Nonclassical Cage Containing Three Heptagons. *Angew. Chem. Int. Ed.*, **2014**, *53*, 2460-2463.
36. Alegret, N.; Abella, L.; Azmani, K.; Rodríguez-Forteza, A.; Poblet, J. M., Different Factors Govern Chlorination and Encapsulation in Fullerenes: The Case of C_{60} . *Inorg. Chem.*, **2015**, *54*, 7562-7570.
37. Gao, C.; Abella, L.; Tan, Y. Z.; Wu, X. Z.; Rodríguez-Forteza, A.; Poblet, J. M.; Xie, S. Y.; Huang, R. B.; Zheng, L. S., Capturing the Fused-Pentagon C_{74} by Stepwise Chlorination. *Inorg. Chem.*, **2016**, *55* 6861–6865.
38. Gao, C.; Abella, L.; Tian, H. R.; Zhang, X.; Zhong, Y. Y.; Tan, Y. Z.; Wu, X. Z.; Rodríguez-Forteza, A.; Poblet, J. M.; Xie, S. Y.; Huang, R. B.; Zheng, L. S., Double Functionalization of a Fullerene in Drastic Arc-Discharge Conditions: Synthesis and Formation Mechanism of $C_{2v}(2)-C_{78}Cl_6(C_5C_{16})$. *Carbon*, **2018**, *129*, 286-292.
39. Martín, N., Fullerene $C_{72}C_{14}$: The Exception that Proves the Rule? *Angew. Chem. Int. Ed.*, **2011**, *50*, 5431–5433.
40. Fowler, P. W.; Manolopoulos, D. E., *An Atlas of Fullerenes*. Oxford Univ. Press, 1995.
41. Kobayashi, K.; Nagase, S.; Yoshida, M.; Ōsawa, E., Endohedral Metallofullerenes. Are the Isolated Pentagon Rule and Fullerene Structures Always Satisfied? *J. Am. Chem. Soc.*, **1997**, *119*, 12693–12694.

42. Qi, J.; Hu, X.; Zhu, H.; Zheng, M., First-Principles Studies on the Structural and Spectral Properties of C_{72} Isomers and the Chlorinated Derivative $C_{72}C_{11}$. *Phys. Chem. Chem. Phys.*, **2016**, *18*, 8049-8058.
43. Tan, Y. Z.; Zhou, T.; Bao, J.; Shan, G. J.; Xie, S. Y.; Huang, R. B.; Zheng, L. S., $C_{72}C_{11}$: A Pristine Fullerene with Favorable Pentagon-Adjacent Structure. *J. Am. Chem. Soc.*, **2010**, *132*, 17102-17104.
44. Ziegler, K.; Mueller, A.; Amsharov, K. Y.; Jansen, M., Disclosure of the Elusive $C_{2v}C_{72}$ Carbon Cage. *J. Am. Chem. Soc.*, **2010**, *132*, 17099-17101.
45. Baerends, E. J.; Ellis, D. E.; Ros, P., *ADF 2013.01; SCM:Amsterdam*, **2013**.
46. Velde, G. t.; Bickelhaupt, F. M.; Baerends, E. J.; Guerra, C. F.; Gisbergen, S. J. A. v.; Snijders, J. G.; Ziegler, T., Chemistry with ADF. *J. Comput. Chem.*, **2001**, *22*, 931-967.
47. Vosko, S. H.; Wilk, L.; Nusair, M., Accurate Spin-Dependent Electron Liquid Correlation Energies for Local Spin Density Calculations: A Critical Analysis. *Can. J. Phys.*, **1980**, *58*, 1200-1211.
48. Becke, A. D., Density-Functional Thermochemistry. III. The Role of Exact Exchange. *J. Chem. Phys.*, **1993**, *98*, 5648-5653.
49. Grimme, S.; Ehrlich, S.; Goerigk, L., Effect of the Damping Function in Dispersion Corrected Density Functional Theory. *J. Com. Chem.*, **2011**, *32*, 1456-1465.
50. Car, R.; Parrinello, M., Unified Approach for Molecular Dynamics and Density-Functional Theory. *Phys. Rev. Lett.*, **1985**, *55*, 2471-2474.

51. Troullier, N.; Martins, J. L., Efficient Pseudopotentials for Plane-Wave Calculations. *Phys. Rev. B*, **1991**, *43*, 1993–2006.
52. Perdew, J. P.; Burke, K.; Ernzerhof, M., Generalized Gradient Approximation Made Simple. *Phys. Rev. Lett.*, **1996**, *77*, 3865–3868.
53. Alvarez-Moreno, M.; de Graaf, C.; López, N.; Maseras, F.; Poblet, J. M.; Bo, C., Managing the Computational Chemistry Big Data Problem: The Iochem-BD Platform. *J. Chem. Inf. Model.*, **2015**, *55*, 95-103.
54. Moreno-Vicente, A.; Mulet-Gas, M.; Dunk, P. W.; Poblet, J. M.; Rodríguez-Forteza, A., Probing the Formation of Halogenated Endohedral Metallofullerenes: Predictions Confirmed by Experiments. *Carbon*, **2018**, *129*, 750-757.
55. Cui, Y. H.; Chen, D. L.; Tian, W. Q.; Feng, J. K., Structures, Stabilities, and Electronic and Optical Properties of C₆₂ Fullerene Isomers. *J. Phys. Chem. A*, **2007**, *111*, 7933–7939.

TOC graphic

